# 2

# Shapes of Delaunay Simplexes and Structural Analysis of Hard Sphere Packings

Alexey V. Anikeenko[1], Marina L. Gavrilova[2], and Nikolai N. Medvedev[1]

[1] Institute of Chemical Kinetics and Combustion SB RAS, Novosibirsk, 630090, Russia
nikmed@kinetics.nsc.ru
[2] Department of Computer Science, University of Calgary, 2500 University Drive NW, Calgary, AB, Canada T2N1N4
marina@cpsc.ucalgary.ca

**Summary.** In this chapter we apply a computational geometry technique to investigate the structure of packings of hard spheres. The hard sphere model is the base for understanding the structure of many physical matters: liquids, solids, colloids and granular materials. The structure analysis is based on the concept of the Voronoi Diagram (Voronoi-Delaunay tessellation), which is well known in mathematics and physics. The Delaunay simplexes are used as the main instrument for this work. They define the simplest structural elements in the three-dimensional space. A challenging problem is to relate geometrical characteristics of the simplexes (e.g. their shape) with structural properties of the packing. In this chapter we review our recent results related to this problem. The presented outcome may be of interest to both mathematicians and physicists. The idea of structural analysis of atomic systems, which was first proposed in computational physics, is a subject for further mathematical development. On the other hand, physicists, chemists and material scientists, who are still using traditional methods for structure characterization, have an opportunity to learn more about this new technique and its implementation. We present the analysis of hard sphere packings with different densities. Our method permits to tackle a renowned physical problem: to reveal a geometrical principle of disordered packings. The proposed analysis of Delaunay simplexes can also be applied to structural investigation of other molecular systems.

## 2.1 Introduction

The 3D structure of an atomic or molecular system is a mutual arrangement of atoms in space. A way to describe this is clear for crystals. A basic structural element (unit cell) and vectors of translation are sufficient for describing the disposition of atoms. It is a common crystallographic approach for structure representation. Aside from that, the investigation of the structural pattern of atom arrangements is also informative for structure understanding. For example, the structure of the densest crystals can be described as a stacking of two-dimensional layers of closely packed atoms. In this case, the distinction between the structure of the hexagonal closed packing (HCP) and the face centered cubic (FCC) crystals appears in different sequences of these layers [AsteW]. For a more detailed description of local structure, the configuration of close groups of atoms is taken into consideration. The crystal packings mentioned above contain two specific local configurations – a regular tetrahedron and a regular octahedron [AsteW, Hales5, Conway88]. In the FCC structure the tetrahedra adjoin by edges

M.L. Gavrilova (Ed.): Generalized Voronoi Diagram, SCI 158, pp. 13–45.
springerlink.com 

forming straight chains, and analogous chains of octahedra are situated between them. On the contrary, HCP contains pairs of face-adjacent tetrahedra (bipyramids), which are absent in FCC.

However, for non-crystalline structures (liquids, glasses, disordered packings of spheres) the question about structural patterns is still open. In these systems there are no obvious local structural elements. Therefore, a way for study the 3D structure is not obvious. A method of correlation functions is traditionally used here [phys_liq, Croxton, Hansen]. The pair correlation function *g(r)* is a more popular characteristic for structure analysis of non-crystalline materials. It represents a "probability" to meet an atom at a distance *r* from a given atom. With the increase of *r,* this function tends asymptotically to unit, and at the distances of a few atomic diameters it demonstrates oscillations meaning a "short distances order" (non-random arrangement of atoms) in dense liquids and glasses. The value of the pair correlation function is that it can be obtained by physical experiments by diffraction of x-rays or neutrons. However, this function contains information only about pair-wise distances between atoms, while the 3D structure of the material is manifested only marginally.

Over the last years, the 3D structure became the main object of investigation for non-crystalline materials. It became possible due to the development of the computer simulation for atomic systems. Computer models of materials represent coordinates of all atoms of a sample. As a result, they can be utilized for detailed analysis of the structure, and not only for calculation of the pair correlation function. On the other hand, experimental methods are developed to obtain coordinates of particles in real physical systems, such as colloids [colloid_exp] and packings of beads [Aste_exp]. However, the question how to extract significant physical information from the arrays of coordinates of atoms remains open. Recent developments in the computer geometry open new possibilities for structure investigation in non-crystalline materials.

The approach proposed here is based on the concept of Voronoi diagrams, which is well known in mathematics and physics [Voronoi, Delaunay, Okabe, Med_book]. For any system of points (ordered or disordered) it is possible to construct a mosaic of polyhedra, which is related in one-to-one manner to the given system of points. Thus, a system of atoms is represented by a collection of discrete elements: Voronoi polyhedra and Delaunay simplexes. One can say that we make a quantization of a system of points in a continuous space. As a result, it becomes possible to use geometrical representation, which helps in description of a 3D structure of atomic systems. In this chapter we utilize only the Delaunay simplexes. Other structural aspects of the Voronoi-Delaunay decomposition (Voronoi polyhedra, Voronoi and Delaunay networks) and their applications to different physical problems are discussed elsewhere [Med_book, Finney70, Malley, Bosticka, Alinchenko, Bryant]. A Delaunay simplex (a quadruple of atoms) is the simplest element of the 3D structure. A cluster of the Delaunay simplexes represents a fragment of the atomic structure. Using this representation one can study structural patterns in an atomic system [Med88, Vol95, Naber91].

A Delaunay simplex can be characterized by its shape. In Section 2.2 we propose different ways to characterize the simplex shape quantitatively. Section 2.3 discusses structural problems of hard sphere packings, which are enjoying a renewed interest in physics. The hard sphere model is widely used for describing structures and phase transitions in simple liquids, amorphous solids and granular materials, but the structure of hard sphere packings itself is still open question. Finally, in Section 2.4 we

demonstrate an application of the proposed technique to computer models of hard sphere pickings, and discuss geometrical principles of disordered packings and the phenomenon of crystallization.

## 2.2 Mathematical Background

### 2.2.1 Delaunay Simplexes

Delaunay simplexes are derived from a fundamental geometrical concept of Voronoi diagram, which is well known in both mathematics and physics [Okabe, Med_book]. The concept exploits an evident geometrical fact that for each atom (point) in a system of atoms (points) it is always possible to distinguish a part of space closest to a given atom. This region is called the *Voronoi region (polyhedron, cell)* and their set, built for all atoms, covering the space without gaps and superposition is called the *Voronoi tessellation*, see Fig.2.1 (thin lines). The Voronoi partitioning defined a dual tessellation for this system, called the *Delaunay tessellation*, which consists of simplexes, whose vertices are the atomic centers, see Fig.2.1 (thick lines). Thus, we have a unified geometrical substance, which is called *Voronoi-Delaunay tessellation* (Voronoi diagram).

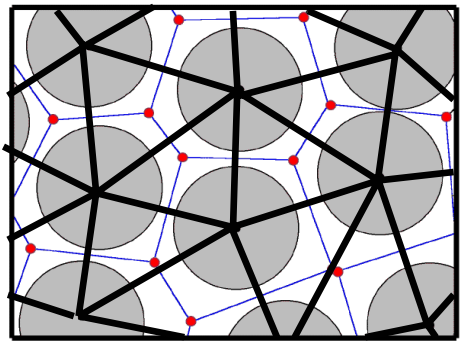

**Fig. 2.1.** 2D illustration of the Voronoi-Delaunay tessellation for a system of identical atoms. Voronoi regions (polygons around the disks, thin lines) determine Voronoi tessellation. Network of edges and vertexes of the Voronoi regions represents Voronoi network of the system (thin lines). Incident atoms to a given Voronoi vertex definea Delaunay simplex (triangles, thick lines). They determine Delaunay tessellation.

Delaunay simplexes were first defined by G. F. Voronoi in his paper [Voronoi] where he considered lattice systems of points. He called them *L*-polyhedra and their tessellation the *L*-decomposition. Later B. N. Delaunay has shown that main properties of *L*-polyhedra that were initially discovered by G. F. Voronoi for lattices, are valid for points that are arbitrary distributed in space [Delaunay]. This fundamental result of B. N. Delaunay opened further broad applications of this geometrical concept to a vast variety of areas [Okabe, Med_book].

The Delaunay simplexes are "bricks" that form an atomic system. As stated earlier, a simplex is the simplest polyhedron in space of a given dimension: it is a tetrahedron of general shape in 3D (Fig. 2.2), and a triangle in 2D. Delaunay simplexes subdivide an atomic system into quadruples of atoms, so any cluster of Delaunay simplexes represents a fragment of the atomic packing (an aggregate of atoms). Thus, if we select Delaunay simplexes with a given structural property, the clusters of such simplexes will reveal a structural pattern reflecting this property in the system. Visualization of spatial distribution of the selected clusters can be easily accomplished within the Voronoi network, which is a network of edges and vertices of the Voronoi regions, see Fig. 2.1. Every site of the Voronoi network is assigned to a Delaunay simplex (it is a circumcenter of the simplex). Every edge of the Voronoi network connecting two neighbor sites corresponds to the two Delaunay simplexes sharing a common face (three atoms that are common). As a result, a cluster of selected simplexes can be represented as a cluster of connected sites on the Voronoi network (see [Naber91] and Section 2.4).

Delaunay simplexes can also be applied for analysis of interatomic voids. By definition of the Delaunay simplex [Delaunay], the inscribed sphere between quadruple of its atoms is empty, i.e. this sphere does not contain any other atoms of the system. Thus, it determines an elementary interatomic cavity. The application of Delaunay simplexes to analysis of empty interatomic space is described elsewhere [Alinchenko, Braynt].

Note that there are different generalizations of Voronoi diagrams [Okabe]. Three of them are used intensively in physics: (i) the classic Voronoi-Delaunay tessellation, which is defined for a set of points (atomic centers) [Voronoi, Delaunay]; (ii) the radical tessellation [Gellatly], which takes the radii of atoms into account (also known as the power tessellation [Aurenhammer87, Gavrilova97], Laguerre tessellation [Telley], or "weighted" Voronoi diagram [Edelsbruner84]); and (iii) the additively-weighted Voronoi diagram [Okabe, Gavrilova]. The latter is also called the Euclidean Voronoi diagram [Okabe, Kim] or Voronoi S-tessellation, because it effectively deals with the surfaces of atoms [Med95, Med06]. To avoid any misunderstanding, we note that in this Chapter we will only deal with the classic Voronoi-Delaunay tessellation, considering the centers of spheres only.

### 2.2.2 The Shape of the Delaunay Simplexes

A measure of shape characterizes its proximity to a given reference shape. There are different ways for estimating such proximity. The mathematical theory of shape characterizes a body by a finite set of points. This theory [Kendall, Small] estimates the proximity of an arbitrary set of points to a given reference set by the degree of coincidence of corresponding points upon superposition. Delaunay simplexes are defined by four points (their vertexes). In this paticular case, a method for shape characterization was implemented in [Anik2006]. However, for simplexes one can use a simpler approach, particularly, the simplex edges can be utilized. In this case an invariant of length edges, which has a zero value for simplex of a reference shape, is constructed. The closeness of this invariant to zero represents the proximity of a given simplex to the template. The problem becomes simpler if a regular tetrahedron

is used as a template. It has identical edges and angles. Using this property of the tetrahedron, various characterizations were proposed: an average variation of the edge lengths [Kimura], the mean of the squares of these variations [Med87], the variation of angles [Debene], the ratio of the circumradius to the volume of the simplex [Med86]. Some specialized characterizations were used for mesh adaptation and mesh optimisation [Dompierre]. The simplest measure for the tetrahedral form was proposed in [Hales97]: it considers the maximum length of the simplex edges. In the next Section, we discuss three different measures, which are used in our work.

#### 2.2.2.1 Edge Length Differences

The *T (tetrahedrisity)* and *Q (quartoctahedrisity)* measures for simplexes were proposed years ago in [Med87] and were used until now [Naber91, Anik_Jap, Brov]. The following invariants of edge lengths are calculated:

$$T = \sum_{i \neq j} (e_i - e_j)^2 / 15 \langle e \rangle^2 . \quad (1)$$

$$Q = \left( \sum_{\substack{i<j \\ i,j \neq m}} (e_i - e_j)^2 + \sum_{i \neq} (e_i - e_m/\sqrt{2})^2 \right) / 15 \langle e \rangle^2 \quad (2)$$

Where $e_i$, $e_j$, $e_m$ are lengths of simplex edges, and <e> is the mean edge length for a given simplex. For a regular tetrahedron (Fig. 2.2a), where all edges are the same, the value of *T* is zero. The value of *T* close to zero indicates unambiguously that a given simplex is close to a regular tetrahedron. A regular quartoctahedron (a quarter of regular octahedron) has one edge √2 times longer than the others, see Fig. 2.2b. The measure *T* for this simplex is not zero, it is approximately 0.05. However, this value of *T* does not determine the quartoctahedron unambiguously, because many distorted simplexes may have the same measure *T*. To define an unambiguous measure for quartoctahedron, we should take into account its peculiarity. It was proposed to use the longest edge $e_m$ of a simplex with a factor of $1/\sqrt{2}$, see equation (2). In a result the perfect quartoctahedron has $Q = 0$. For an almost perfect quartoctahedron the value of *Q* approaches zero.

Another interesting simplex is the flat simplex (two opposite edges are √2 times longer then the others), see Fig. 2.2c. This simplex is important for analysis of dense packing of spheres. At a random distortion of a regular octahedron (Fig. 2.2d), it is normally subdivided into four quartoctahedra. However, at a certain displacement of the vertices, it can be subdivided also into five simplexes [Vol89]: four of them are quartoctahedra, while the fifth one, which is determined by four atoms at the middle plane of octahedron, looks like a square. Such subdivision is fairly uncommon; it is caused by two atoms on each end of the diagonal of the square being elevated above the equatorial plane (in [Vol89] such simplex was named the *Kizhe simplex*). The

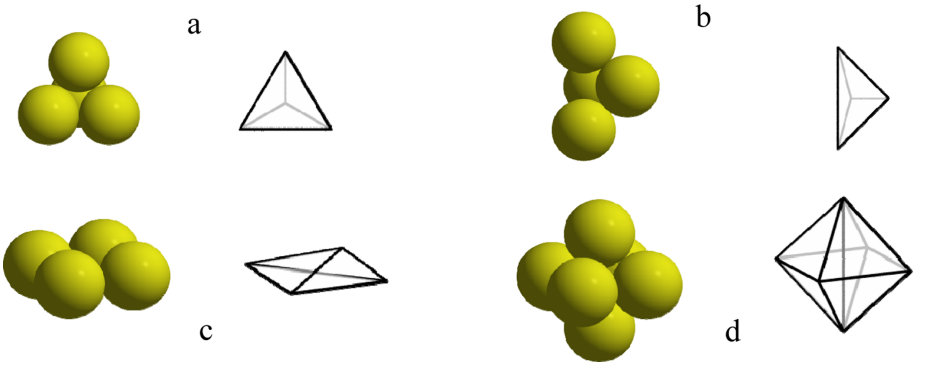


**Fig. 2.2.** (a) – a regular tetrahedron; (b) – a regular quartoctahedron (one edge √2 times loner then other ones); (c) – a flat simplex with a shape of a square; (d) – a perfect octahedron. The octahedron is divided by infinitesimal perturbations on four quartoctahedra or four quartoctahedra and one flat simplex [Vol89].

regular square "simplex" has two opposite edges that are √2 times longer than the other four edges. Similarly to (2) we can write:

$$K = \Big(\sum_{\substack{i<j \\ i,j\neq}} (e_i - e_j)^2 + \sum_{i\neq m,n} (e_i - e_m/\sqrt{2})^2 + \sum_{i\neq m,n} (e_i - e_n/\sqrt{2})^2 + (e_m - e_n)^2\Big)/15\langle e\rangle^2 \qquad (3)$$

Thus, a degenerate (square) simplex has $K = 0$, and at small distortions the value $K$ is also small. In order to compute this measure, the edges $m$ and $n$ are selected as a pair of the longest opposite edges of a simplex. Note these "virtual" simplexes can be important for the analysis of clusters of the Delaunay simplexes, for example for studying crystalline nuclei. In this case connectivity of the simplexes is taken into account. Neglecting these simplexes can result in a loss of integrity of slightly distorted octahedral configurations.

Following the idea of the formula (3), one can define measures to select simplexes of other specific shapes. The Delaunay simplex of the body centered cubic lattice (BCC) is one of the important simplexes for dense packings. In this simplex, the two opposite edges of the simplex are $2/\sqrt{3}$ times longer then the others.

The proposed measures should be calibrated before their application. A calibration of these measures has been done in [Med87, Naber91, Anik_Jap], utilizing models of a known structure (slightly distorted FCC crystal). It was proposed to use the value of $T_b = 0.018$ as a boundary to select the class of tetrahedra (simplexes closer to the regular tetrahedron), and $Q_b = 0.014$ to select the class of quartoctahedra (simplexes closer to the regular qurtoctahedron) [Anik_Jap]. These boundary values seem reasonable in application to packings of hard spheres as well [Anik2006]. Indeed, the value $T_b$ corresponds to a minimum on the $T$-distribution for crystalline packings of

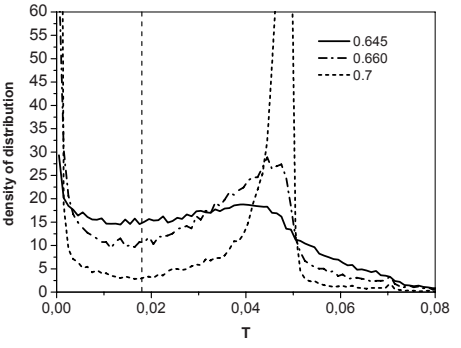


**Fig. 2.3.** T-distributions for packings of hard spheres with different packing fractions: 0.70 (well crystallized); 0.660 (partly crystallized);0.640 (disordered). Dashed vertical line (T=0.018) shows a border for the family of simplexes with quasi-regular tetrahedral shape.

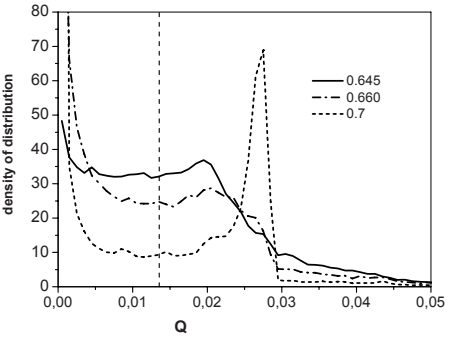


**Fig. 2.4.** Q-distributions for the same packings. Dashed vertical line (Q=0.014) shows a border for the family of simplexes with quasi-regular quartoctahedral shape.

hard spheres, see Fig.2.3. Similarly, the value $Q_b$ corresponds to the minimum in the $Q$-distribution, see Fig.2.4.

For higher density crystalline structure (0.70), the $T$- and $Q$-distributions demonstrate clear separated peaks. It means, a majority of Delaunay simplexes converges to these two perfect forms. The peak at $T=0$ in the Fig. 2.3 corresponds to the tetrahedra, and the peak at $T=0.05$ corresponds to the quartoctahedra. In much the same manner the peak at $Q=0.028$ in the Fig. 2.4 represents tetrahedra. Disordered packings (0.64) have a smoother spectrum of simplex shapes, however, the maxima for $T$ and $Q$ are also recognizable.

#### 2.2.2.2 Procrustean Distance

In mathematical shape theory, the proximity of an arbitrary simplex to a given referenced shape is estimated by the degree of coincidence upon their superposition [Kendall, Small]. Here, the total mean square deviation $d^2$ between the corresponding vertices of the optimally superimposed simplexes is calculated. The magnitude of $d$ is called the *Procrustean distance* between the two simplexes. Let $\{\mathbf{x}_1, \mathbf{x}_2, \mathbf{x}_3, \mathbf{x}_4\}$ and $\{\mathbf{y}_1, \mathbf{y}_2, \mathbf{y}_3, \mathbf{y}_4\}$ be the vertices of two simplexes in three-dimensional space. The square of Procrustean distance between two simplexes is computed as

$$d^2 = \min_{\mathbf{R},\mathbf{t},P} \left\{ \frac{1}{4} \sum_{i=1}^{4} \left\| \mathbf{y}_i - (\mathbf{R}\mathbf{x}_i + \mathbf{t}) \right\|^2 \right\}$$

where the minimum is calculated over all 3D rotations **R,** translations **t,** and all possible mappings between vertices of the simplexes ***P***. Despite the seeming complexity of

this measure, the problem has been solved analytically, and the computation of the Procrustean distance is not much more difficult than the computation of the *T* or *Q* measures. There are several algorithms for analytical solution of the least squares problem at a defined correspondence between vertices (mapping) [Dryden, Eggert]. One of the most efficient methods is based on computing the singular value decomposition of the derived matrix [Umeyama]:

$$d^2 = \begin{cases} \sigma_x{}^2 + \sigma_y{}^2 - 2(d_1 + d_2 + d_3), & \text{if } \det(\boldsymbol{\Sigma}_{xy}) \geq 0 \\ \sigma_x{}^2 + \sigma_y{}^2 - 2(d_1 + d_2 - d_3), & \text{if } \det(\boldsymbol{\Sigma}_{xy}) < 0 \end{cases}$$

where, $\sigma_x{}^2 = \frac{1}{4}\sum_{i=1}^{4} \|\mathbf{x}_i - \mathbf{x}_c\|^2$ and $\sigma_y{}^2 = \frac{1}{4}\sum_{i=1}^{4} \|\mathbf{y}_i - \mathbf{y}_c\|^2$ are variances around centroids of simplexes $\mathbf{x}_c = \frac{1}{4}\sum_{i=1}^{4} \mathbf{x}_i$ , $\mathbf{y}_c = \frac{1}{4}\sum_{i=1}^{4} \mathbf{y}_i$ ,

$\boldsymbol{\Sigma}_{xy}$ is a covariance matrix $\boldsymbol{\Sigma}_{xy} = \frac{1}{4}\sum_{i=1}^{4} (\mathbf{y}_i - \mathbf{y}_c)(\mathbf{x}_i - \mathbf{x}_c)^T$

and $d_1 \geq d_2 \geq d_3 \geq 0$ are singular values of matrix $\boldsymbol{\Sigma}_{xy}$.

There is no natural correspondence between vertices of different simplexes. Thus, the value $d^2$ is calculated for all possible mappings between vertices of two simplexes and the minimal value is taken as the distance between them. The amount of calculations on this step can be reduced due to the symmetry of the referenced simplex. In particular, we may skip permutations of vertices that correspond to the same rotational subgroup of the referenced simplex.

Table 2.1 shows the Procrustean distances *d* between regular simplexes inherent to FCC, HCP and BCC crystalline structures with unit sphere diameter.

Table.1. Procrustean distances between regular simplexes of some specific shape.

**Table 1.**

| | *Tetrahedron* | *Quartoctahedron* | *Square* | *bcc simplex* |
|---|---|---|---|---|
| Tetrahedron | 0 | 0.17936 | 0.40975 | 0.10096 |
| Quartoctahedron | 0.17936 | 0 | 0.28974 | 0.11360 |
| Square | 0.40975 | 0.28974 | 0 | 0.31650 |
| bcc simplex | 0.10096 | 0.11360 | 0.31650 | 0 |

Note that the Procrustean distance is a well defined distance measure, mathematically speaking, i.e. the distance between two equivalent simplexes is zero, and the distance measured from simplex *i* to simplex *j* is the same as the distance from *j* to *i*.

Note if we have a set of reference simplexes, we can compute which shapes of simplexes are closer to these reference simplexes. Thus formally, one can define a "Voronoi region" for a given reference simplex. This region contains simplexes whose Procrustean distances are shorter to a given one then to any other simplex from the given set. It is an interesting generalization of Voronoi diagram on the "space of simplexes." However, it is not clear this observation can be utilized for solution of the discussed structural problems.

It was discussed in [Anik2006] that distributions of the Procrustean distances of Delaunay simplexes to regular tetrahedron $d_T^2$ and regular quartoctahedron $d_Q^2$ in packings of hard spheres are very similar to corresponding distributions of $T$ and $Q$ measures shown in Fig. 2.3 and Fig. 2.4. However, the Procrustean distance also requires calibration. It seems natural to take the half of the Procrustean distance between tetrahedra and quartoctahedra as a boundary between them, see Table 2.1:

$$d^b_T = d_{TQ}/2 = 0.0897. \tag{4}$$

Another criterion to select tetrahedra was proposed in [AnikPRL]:

$$d_T < d_Q. \tag{5}$$

Here, a simplex is considered as a tetrahedral one if its Procrustean distance to the regular tetrahedron is shorter than the distance to the regular quartoctahedron. Note the condition (5) takes into account more disordered simplexes then the condition (4). Fig. 2.5 contains a spot $d_T$ - $d_Q$ diagram for the Delaunay simplexes. Every point on the diagram represents a Delaunay simplex in a packing of hard spheres. The abscissa of the point is the value of Procrustean distance of the given simplex to the regular tetrahedron ($d_T$ ), and the ordinate is its distance to the regular quartoctahedron ($d_Q$). The packing consists of 10000 hard spheres, whose Delaunay decomposition contains of approximately 61000 simplexes (see Section 2.4 for details).

The specific border of area occupied by points in Fig. 2.5 and their condensation inside the diagram reflect specific features of Delaunay simplexes in packings of hard spheres. It can be proven that a straight line between regular tetrahedron and regular quartoctahedron (connecting points with coordinates (0.0, 0.17936) and (0.17936, 0.0) ) corresponds to simplexes which have five edges equal to 1 (the diameter of a hard sphere). The sixth edge is longer, and it changes from 1 to $\sqrt{2}$ along the given segment. Such simplexes were called *isopentakmones* in [Vol89]. This set of simplexes covered a sufficient part of Delaunay simplexes of dense packings of hard spheres. It means the spheres forming Delaunay simplexes are usually touching each other in such systems. The continuation of the straight line from point (0.17936, 0.0) in direction of increasing $d_T$ also corresponds to isopentakmones. However, in this case the sixth edge is larger then $\sqrt{2}$. As one can see, they are marginal in the dense packing.

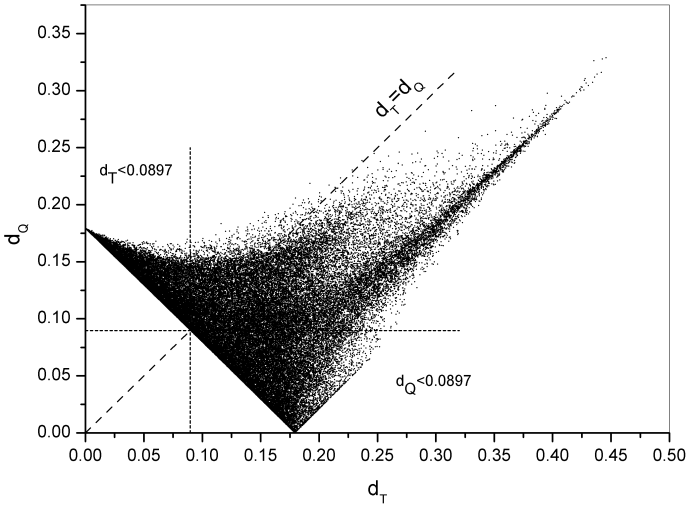


**Fig. 2.5.** Scatter $d_T$ - $d_Q$ diagram for a packing of hard sphere with density $\eta$=0.64. Dashed lines show border for tetrahedral simplexes according criterion $d_T < d_Q$. Dotted lines show criteria $d_T < 0.897$, and $d_Q < 0.897$.

A narrow "ridge" going to the upper- right corresponds to simplexes that have four edges of unit length, and the other two edges are longer. This class of simplexes can be called *isotetrakmones.* The Kizhe simplex mentioned above belongs to this class. It corresponds to a point in the diagram with the coordinates (0.40975, 0.28974), see Table 2.1.

The Procrustean distance and the measures *T* and *Q* estimate simplexes differently. The former uses vertexes, while the latter uses edges, which do not define the simplex exactly. Indeed, the same set of edges can be arranged in different manners. Fig. 2.6 demonstrates an example for set of simplex edges {1, 1, 1, 1, √2, √2}. If the longer edges are opposite of each other, then the simplex degenerates to a flat square. If the longer edges meet at a common vertex, the simplex gets another shape. The values of measure *T*, obviously, are the same for both simplexes, but the Procrustean measures are different.

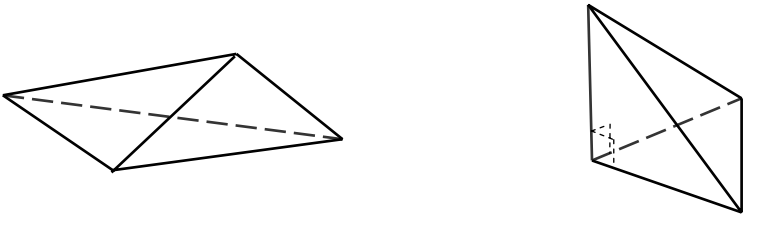

**Fig. 2.6.** An example of two different simplexes with the same set of edge lengths {1,1,1,1,√2, √2} and different arrangement: the longer edges are opposite (left), and the longer edges have a common vertex (right).

Thus, simplexes with identical values of $T$ can have various $d_T$, and vice versa. It is not surprising since any scalar shape measure of a three-dimensional object cannot be well-defined. However, if simplexes are close to a reference shape, then correlation between the measures becomes better, i.e. the shape can be recognized by its edges as well as by its vertices.

#### 2.2.2.3 Hales' Quasi-regular Tetrahedra

To find out whether a simplex is tetrahedral it may be sufficient to calculate the length of the maximal edge $e_{max}$. This approach seems especially suitable for identical hard spheres, where the diameter of the sphere sets the minimal possible length of the simplex edge as 1. A convenient measure of the simplex shape is then the difference between the lengths of the maximal and the minimal edges: $\delta = e_{max} - 1$. Smaller values of $\delta$ unambiguously indicate that the shape of the simplex is close to perfect tetrahedron, while larger values mean substantially distorted shapes. This method for selecting tetrahedral simplexes was used by Hales in his work on proving the Kepler conjecture [Hales5, Hales97]. As a boundary measure for such simplexes, Hales chose the maximal edge length of *2.51* of the radius of the sphere. In our notation it corresponds to $\delta = 0.255$. He found this boundary by trial, and named the class of selected simplexes the "quasi-regular tetrahedra". We will also use also this boundary, i.e. a simplex is considered to belong to the family of tetrahedra if it satisfies condition [AnikPRL]:

$$\delta < 0.255 \tag{6}$$

Fig 2.7 illustrates the geometrical meaning of the Hale's tetrahedra. They present the most locally dense configurations. The location of the empty inscribed sphere is shown for simplexes of different shapes. The hard spheres of unit diameter centered at the simplex vertexes are not shown. For the perfect tetrahedron (δ=0) the inscribed sphere lies completely inside the simplex. This holds for value up to δ=0.20, and at δ=0.255 only 10% of the sphere lies outside the simplex. Thus, the class of Hales'

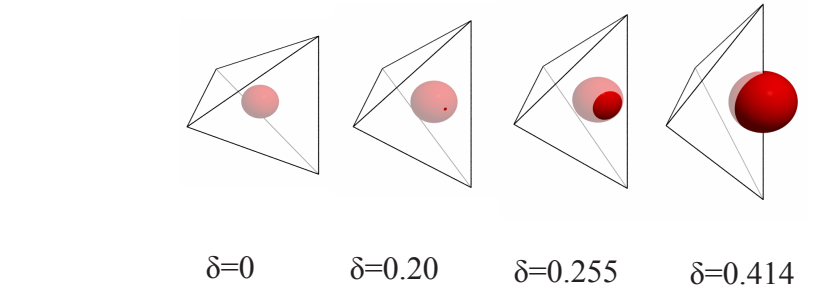


**Fig. 2.7.** Location of empty inscribed sphere in simplexes of different shape. The sphere is inscribed between four hard spheres of unit diameter centered on the vertexes of the simplexes (do not shown). For perfect tetrahedron, δ=0, inscribed sphere is in the depth of simplex (left). For perfect quartoctadron, δ=0414 the sphere is on 3/4 outside of the simplex (right). For simplex with δ=0.20 the inscribed sphere is still inside the simplex. For simplex with δ=0.255 (Hales' border) the inscribed sphere go out only on 10%.

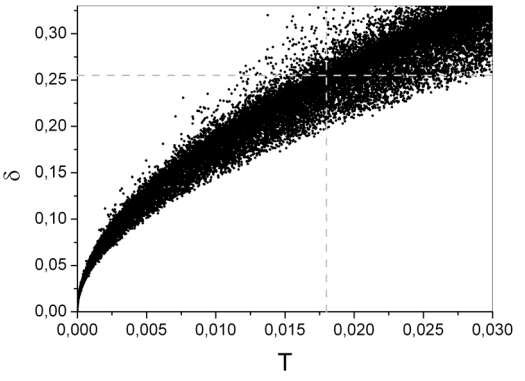


**Fig. 2.8.** Correlation δ-T diagram for packing f hard sphere with density 0.64. Dashed lines show borders for simplexes of tetrahedral shape: T<0.018 and δ < 0.255.

thetrahedra presents compact configurations of spheres. For the perfect quartoctadron (δ=0.414) 3/4 of the inscribed sphere lies outside of the simplex. Such the configurations where the simplex does not present "an individual cavity" are typical for disordered simplexes.

It is interesting to note that in dense packings of hard spheres all of the described measures with indicated boundaries classify practically the same Delaunay simplexes into the class of tetrahedra. For example, in disordered packing with packing fraction of 0.64 the conditions $T<0.018$ and $\delta<0.255$ classify 90% of simplexes the same way. The correlations between the measures are shown in Fig. 2.8. The points correspond to Delaunay simplexes, and their coordinates are measures $T$ and $\delta$ of every simplex. Unlike of Fig. 2.5, only the region nearby the origin of the coordinate system is shown. The vertical and horizontal lines represent the proposed boundaries of tetrahedra classification. Note that density of points on the diagram increases to a spike, which represents a good correlation between $T$ and $\delta$ in this region.

### 2.2.3 Structural Types of Delaunay Simplexes

The structural transformation of matter during crystallization, aging, and relaxation processes is an important problem in material science. The structural heterogeneity is a feature in such processes. In other words, a sample can contain regions of different structures, both crystalline and disordered. It is not an easy task to investigate such structures. It requires development of special approaches. In [Anik_LNCS, Anik_ZSX] we proposed a method for revealing regions (nuclei) of crystalline structures, based on the shape of Delaunay simplexes and their mutual arrangement.

#### 2.2.3.1 A Structural Unit

The shape of Delaunay simplexes cannot be applied immediately for some particular structural problems. First of all, the shape of an individual simplex, as a rule, does not characterize the structure uniquely. For example, a tetrahedron can belong to both FCC and HCP structures, and it can also be found in amorphous phase. On the other hand, a crystal structure is not always represented by one type of simplexes. In

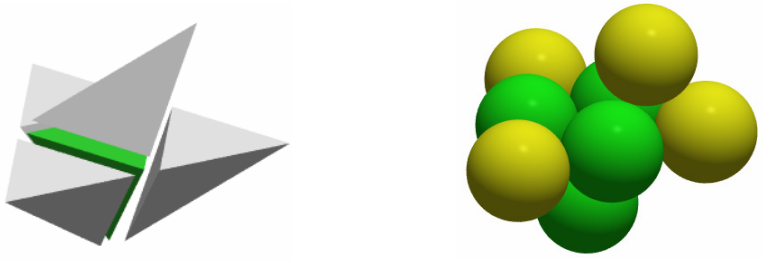

**Fig. 2.9.** Illustration of a structural unit determinated structural type of Delaunay simplex. Four face-adjacent simplexes are taken into account (left). The corresponding aggregate of atoms (right). The central simplex is show by green atoms, its neighbors are yellow.

particular, as it was mentioned above, the most dense crystalline structures consist of Delaunay simplexes of three different shapes: tetrahedral, quartoctahedral and simplexes close to a flat square, see Fig. 2.2. The differences between the FCC and HCP crystals are characterized by the mutual arrangement of these simplexes.

In [Anik_LNCS] we suggested to characterize the relationship of simplexes to the structure by considering the shape of a given simplex together with the shapes and the arrangement of its neighbors. We refer to this process as the identification of the *structural type* of a Delaunay simplex. When considering neighbors we only look at simplexes with adjacent faces. In this case, the structural unit is an aggregate of eight atoms: four atoms of a given simplex and four atoms at its faces. Fig. 2.9 is an example of a tetrahedral simplex (located in the center) inside FCC structure, i.e. this simplex has the FCC type. The face-adjacent neighbors of this simplex are quartoctahedra, see below.

Note that our method, which only accounts the four face-adjacent neighbors, is a first order approximation. In principle, it can be expanded to consider also edge-connected simplexes. However, the simplest variant turns out to be very productive.

#### 2.2.3.2 Crystal types

It is easy to see that in FCC crystal every tetrahedral configuration is adjacent over faces only to octahedra, and every octahedral configuration is adjacent only to the tetrahedra. In terms of the Delaunay simplexes, this represents the following combinations of the neighboring simplexes:

$$\begin{aligned} &\text{(I)}\ \ T{:}\ \ Q\,Q\,Q\,Q \\ &\text{(II)}\ \ Q{:}\ \ T\,T\,Q\,Q \\ &\text{(III)}\ \ Q{:}\ \ T\,T\,Q\,K \\ &\text{(IV)}\ \ K{:}\ \ Q\,Q\,Q\,Q. \end{aligned} \tag{7}$$

Thus, a tetrahedral Delaunay simplex may be adjacent to four quartoctahedra (I). A quartoctahedron can be adjacent to two tetrahedra and two quartoctahedra (II) or to two tetrahedra, one quartoctahedron and one flat simplex (III). The flat simplex can be adjacent only to four quartoctahedra (IV).

Thus, a given Delaunay simplex can identify the FCC structure if it satisfies one of the conditions (7). Cases (III) and (IV) arise when the division of an octahedron into Delaunay simplexes contains flat simplexes Kizhe, see Fig. 2.2.

The HCP structure contains pairs of adjacent tetrahedra (trigonal bipyramids), and the octahedra are organized in chains, where they are also adjacent by faces. Thus, one can derive the following set of neighborhoods of the Delaunay simplexes:

$$\begin{aligned}
&\text{(I)}\ T{:}\ T\,Q\,Q\,Q\\
&\text{(II)}\ Q{:}\ T\,Q\,Q\,Q\\
&\text{(III)}\ Q{:}\ T\,Q\,Q\,K\\
&\text{(IV)}\ Q{:}\ T\,T\,Q\,Q\\
&\text{(V)}\ Q{:}\ T\,T\,Q\,K\\
&\text{(VI)}\ K{:}\ Q\,Q\,Q\,Q
\end{aligned} \tag{8}$$

Combinations (I)-(III) are new ones, while (IV)-(VI) are the same as for FCC, see Fig.2.6. The similarity of some combinations is not surprising due to the genetic proximity of the most dense crystalline structures. Thus, the classification of crystalline simplexes into FCC and HCP may be somewhat ambiguous. The classification of the "disputed" Delaunay simplexes requires additional consideration. The number of these questionable Delaunay simplexes can be decreased by some further analysis of the model. Indeed, if for instance a disputed simplex is adjacent to simplexes of a given type, then it can also be classified into this type. This consideration can help to reduce the number of disputed simplexes. Thus, if a simplex only has the FCC type simplexes among its neighbors, and does not have any HCP-type neighbors, then it is assigned to the FCC type. Analogously, if a disputed simplex is surrounded by simplexes of the HCP type and none of the FCC type, then it is classified as HCP type. However, if a disputed simplex is adjacent both to FCC and HCP types, it is still considered as disputed. Such case can be observed at the border between FCC and HCP nuclei. Note that the disputed simplexes, nevertheless, represent the "crystalline phase." We keep simplexes as disputed also if they do not have neighbors of either FCC or HCP types, which can happen for small aggregates in the disordered phase.

We can also define another structural type, e.g. BCC (body centered cubic). Here, we should first select a class of simplexes with shapes close to the shape of Delaunay simplex of the BCC lattice. Let us mark such simplexes as *B*. Since the BCC lattice consists of only one type of simplexes, the rule to assign the BCC type to a simplex is very simple:

$$\text{(I)}\ B{:}\ B\,B\,B\,B \tag{9}$$

Thus, after selecting such Delaunay simplexes in the model we obtain information about the presence of BCC structures in the sample.

#### 2.2.3.3 Non-crystal Types

This approach can be also applied to extraction of non-crystal local structures. Aggregates of face-adjacent tetrahedra that is typical for dense amorphous phase [Bernal64], are of particular interest. The arrangement of more than two tetrahedra is extraneous to lattices, since they are incompatible with translational symmetry. Thus for selecting such configurations, one should extract Delaunay simplexes with a tetrahedral shape having at least two tetrahedra in its neighborhood:

$$\mathrm{T}: \ \mathrm{T}\ \mathrm{T}\ *\ *. \tag{10}$$

The other neighboring simplexes can have an arbitrary shape in general. Polytetrahedral clusters, and, particularly, five-membered rings of tetrahera (pentagonal bipyramids), can be identified by this structural type.

## 2.3 Structural Problems in Hard Sphere Packings

The structure and the degree of disorder in hard spheres packings depend heavily on the density. The maximal packing fraction of identical hard spheres ($\pi/\sqrt{18} = 0.74$) is attained only in a perfect crystalline structure (FCC, HCP or their mixture [AsteW]). This fact (the Kepler conjecture) was known for many years, but it was proven only recently [Hales5]. Another famous value of density is Bernal's limiting density, which is approximately 0.64. It is a limit for non-crystalline packings (which is also called "close random packing" in the literature). This phenomenon was discovered experimentally almost a half century ago [Bernal59, Bernal60, Bernal64], but it did not receive a compelling explanation until now. The density at around 0.55 is a low limit for disordered packings of spheres (loose random packing) [Onoda]. It corresponds to a rigidity percolation threshold for disordered packings of spheres: the non-crystalline packing cannot exist at a lower density. However, these values of density do not exhaust all possible changes of the packing structure. Modifications of the structure, which happen at intermediate densities, are also very interesting. Experimentally, the following properties of packings of identical spheres are established [Aste05]. Reversible structures can be created at 0.61–0.62 density by pouring grains into a container and tapping for sufficiently long time. To reach the density 0.63–0.64, not only tapping but also some combined compression must be added. More dense packings contain crystalline regions inevitably.

The structure of hard sphere packings at different densities is a broad field of research for physicists and mathematicians alike. Below, we discuss some recent structure problems in more details.

### 2.3.1 The Principle of Structural Organization of Non-crystalline Pickings

J. Bernal was the first to study the structure of disordered hard sphere packings [Bernal64]. An important outcome of his research was a realization that dense disordered packing of spheres is an independent structural object: it cannot be considered random, as it demonstrates substantial correlations, but on the other hand, it is not a perturbed crystal. Bernal has shown that disordered packings contain a large fraction of tetrahedral configurations of spheres. In such packings, the tetrahedra tend to unite

in aggregates by their faces. A further study of computer models confirmed that the tetrahedra have a tendency to make branched lineal clusters of face-adjacent tetrahedra and to form 5-member rings, which are absent in crystal structures [Finney70, FinneyW, Med90]. The recent results obtained on large computer models verify this and advance our understanding of the nature of disordered structure [AnikPRL, AnikPRE]. Now, one can say definitely that the main feature of dense disordered packing of spheres is the existence of polytetrahedral clusters, i.e. aggregates of face-adjacent tetrahedral configurations of spheres. These aggregates present nuclei with high local density atypical for crystal structures. It can explain as the comparative stability of supercooled liquids [Frank], as well as the results of diffraction experiments on simple liquids [Reichert, Schenk]. Thus, one can speak about a "polytetrahedral" principle of structure of dense disordered packings. We illustrate this conclusion below.

However, the nature of the non-crystalline structure is not yet completely understood. Polytetrahedral aggregates occupy not more than one-third of the sample, while the other 2/3 of the packing are out of consideration. Complementarities of these regions with polytetrhedral aggregates are a subject of further investigation.

### 2.3.2 The Origin of the Bernal's Limiting Density

Physical experiments provide an estimate of 0.637 - 0.64 for the Bernal's limiting density [Bernal64, Aste05, Scott69]; and various computer simulations provide approximately the same values [Jodrey, Clarke, Rintoul]. Recently, this density was estimated as ~0.646 using sensitive structure parameters based on Delaunay simplexes [Med2006, AnikPRL]. It is an important fact that these values are substantially lower than the maximum packing fraction attainable in the most dense crystalline structures 0.74. The origin of the Bernal's limiting density and its precise value are not known today despite the substantial effort that has been put into this research. A complexity of the problem lies in the difficulty of mathematical formulation of the problem, and until now no adequate quantitative definition of the densest disordered packing was proposed [Torquato2000]. This problem seems as engaging and important as the Kepler conjecture on the most dense crystalline packing of spheres [Hales5].

A step to understanding the reason of Bernal's limiting density was made recently in [AnikPRL, AstePRE], where the following question was raised: which characteristic of the packing is exhausted to the limiting density when it becomes impossible to make a denser packing while keeping a principle of non-crystalline structure. We discuss it in more detail below.

### 2.3.3 Are There Other "Critical" Densities Besides 0.74, 0.64, and 0.55?

Are there other values of density (besides the above-mentioned "critical" densities) where some non-trivial structural changes take place? Until now, the question is open. Note we consider only the mathematical aspect of the sphere packing problem. Any physical reasons like friction coefficient between the spheres, gravitation, which can influence the structure, are not considered here. A packing fraction 0.60 arouses suspicion. Indeed, it is difficult to obtain packing of spheres with densities less than 0.60 experimentally [Scott69, Aste05, Onoda]. A loose random packing with density of

0.555 was obtained using glass spheres immersed in liquids with adjusted densities [Onoda]. One can think that the specific value of 0.60 relates only to gravitation. However, this value is also noticed in computer simulation. In particular, it is impossible to get denser packing using standard methods of computer simulation like molecular dynamics [Richard99]. The specifics of this density value may relate to the additional structural correlations in the packing, which arise to surmount this value of density [ZSX07].

Another interesting value (0.66) was mentioned in [Med2006, Kristin]. It concerns the problem of filling the space by crystalline nuclei. Note that crystal areas appear in the packing once it passes Bernal's density. Densities in the interval 0.64-0.66 are achieved by inclusion of crystal nuclei, which are independent from each other. With the increase of density, crystalline areas occupy more and more volume in the packing and cohere into total crystal at around 0.66. This value of packing fraction was also notes in [AstePRE]. The structural entropy of the packing begins a linear decay to zero toward the densest crystalline packing after this point. The quantitative analysis of this phenomenon needs further investigations.

### 2.3.4 Statistically Preferable Configurations

The structure of a packing depends on its density. However, a given density can be realized in an infinite number of ways. Even the maximal packing fraction 0.74 is realized not only by HCP and FCC structures, but also by an uncountable set of packings where the basic 2D close packed planes are stacked randomly [AsteW]. For disordered packings the situation aggravates, as any density can be realized by massive set of various configurations. Besides homogeneous packings, inhomogeneous packings are also possible. It is known that liquid phase can coexist with crystal, glasses can contains crystal nuclei, and conversely, disordered regions can exist in a crystal. In physics such structures are usually unstable and turn with time into a crystal, which is more preferable from thermodynamics point of view. Moreover, formally any value of density can be obtained easily from the densest crystal packing. It is enough to remove the required number of atoms from the crystal. Furthermore, one can envision a large number of other specific ways to arrange atoms in space with a given density. This indicates that we should understand clearly which kind of structures we study. Obviously, any peculiar configurations are not too interesting for physics.

In this work we deal with a class of models, which can be called *statistically preferable models for a given density.* We do not try to give a mathematical definition for this notion and use it as intuitively understood. Pouring of balls into a container and computer generated packing, starting from a random configuration of spheres, belong to this class of packings. In our previous research we called such kind of packings as "more disordered at a given density" [Kristin, AnikPRL]. The "disorder jammed" packings discussed in [Torquato2000] are also close to this class of models.

Thus, we are passing over theoretical manifolds of possible configurations realizing a given value of density and only considering a more preferable filling of space by spheres. Thus, it is not so important how such packing is created. A crucial problem is to understand which kinds of the more statistically probable configurations correspond to a given density.

## 2.4 Analysis of Hard Sphere Packings

The hard sphere model is used widely in structure studies of liquids, glasses, colloids, and granular materials. It successfully reproduces the main properties of the condensed phase, such as crystallization of liquids [Hoover, Auer] and glass transition [Clarke, Rintou]. The wide applicability of this simple model reflects the fact that the structure of dense matter is determined primarily by mutual impenetrability of atoms, and ultimately comes from geometric properties of the packings of spheres in three-dimensional space [Bernal64]. However, the structure of hard sphere packings itself is still open question. Here we present results of our recent investigations of computer modes of hard sphere packings at different densities.

### 2.4.1 Computer Models of Hard Spheres

We consider a set of hard sphere packings obtained in our recent research [Kristin, AnikPRL]. Each packing contains 10000 identical hard spheres in a model box with periodic boundary conditions. More than 200 packings with density from 0.53 to 0.71 were obtained using a modified Jodrey-Tory algorithm that employs "repulsion" of overlapping spheres with gradual reduction of their radii [Jodrey, Kristin]. This algorithm can easily produce disordered packings with densities up to the limiting value ~0.64, as well as denser systems containing crystalline structures. To test the

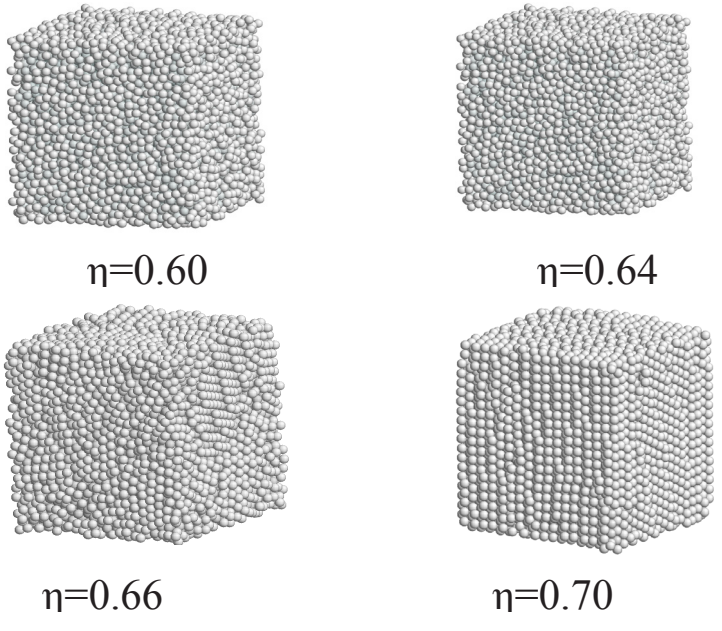


**Fig. 2.10.** Computer packings of hard spheres with different packing fraction. 10000 identical spheres with the periodic boundary conditions.

independence of structure on the packing generation algorithm we also constructed a series of 70 packings in the range of densities from 0.54 to 0.67 using the Lubachevsky-Stillinger algorithm [Skoge]. This algorithm employs a different procedure for raising the density: a molecular dynamics of non-overlapping spheres with gradual increase of their radii.

All our packings can be considered to be "statistically preferable at a given density" (see Section 2.3.4). To generate these packings, we start from a random initial configuration of spheres, and using the quickest way to "lead" it to the desired density. This is fairly easy to achieve by an appropriate choice of algorithm parameters [AnikPRL, AstePRE]. As a result, for densities below the limiting value 0.64 the disordered packings are always produced. Crystallization naturally begins at higher densities, see Fig. 2.10.

Additional analysis shows that independent packings with the same density demonstrate similar structure, i.e. the pair correlation functions and standard statistical characteristics of the Voronoi polyhedra and Delaunay simplexes are practically identical for such packings. The representativeness of our models is further illustrated by a fairly good coincidence of points for each given density value in figures below, where each point represents an independent packing.

### 2.4.2 Pair Correlation Function

Before considering Delaunay simplexes, let's examine the traditional structure characteristic, the pair correlation function *g(r)*. Fig. 2.11 demonstrates this function for packings at different densities. For dense disordered packings, it depends only weakly on density: for packing density 0.62 to 0.64 the pair correlation function looks almost identical, see Fig. 2.11, at the bottom.

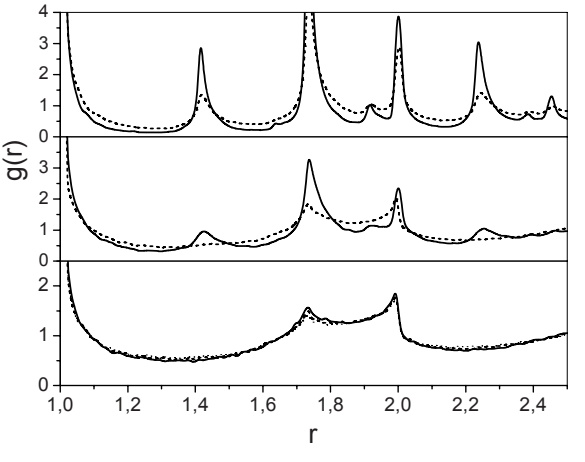


**Fig. 2.11.** Pair correlation function of hard sphere packings with different densities
bottom — 0.62 (dots), 0.64 (solid);
middle — 0.65 (dots), 0.66 (solid);
top — 0.67 (dots), 0.70 (solid).

At the density 0.65 the pair correlation function still looks like disordered. Nevertheless, as we will show below, this packing contains a visible amount of crystalline embryos. This *g(r)* has low sensitivity to the beginning of crystallization. At density 0.66 the sharp peaks pop up. One can see a clear maximum at *r ~1.41* (the diagonal of the quadrangle configuration of atoms), which is commonly believed to be the first signature of the crystalline structure. The second peak at *r~1.73* is also attributed to the HCP and FCC structures, see Fig. 2.11, middle. At higher densities the crystal structure of the packings is cogent, with many crystalline distances become very pronounced; see Fig.2.11, on the top.

Thus, the pair correlation function reveals fundamental changes occurring during densification. However, many features of the structure transformation remain concealed.

### 2.4.3 Tetrahedra and Quartoctahedra

For each packing of our set of models we calculated Delaunay simplexes and picked those that had a given specific shape. Here we consider classes of tetrahedra and quartoctahedra, which are determined according the conditions discussed in Section 2.2.

Fig. 2.12 shows how the fraction of tetrahedra $n_T$ depends on the density of the packing. It can be seen that the general behavior of the curves is similar for all three measures that can be used to characterize select simplexes of this family, as proposed in Section 2.2.

The fraction of tetrahedra grows rapidly with increasing density, reaching ~30% when approaching the critical value of ~0.64. Thus, we confirm the accepted qualitative conclusions that the dense disordered packings of spherical atoms contain many

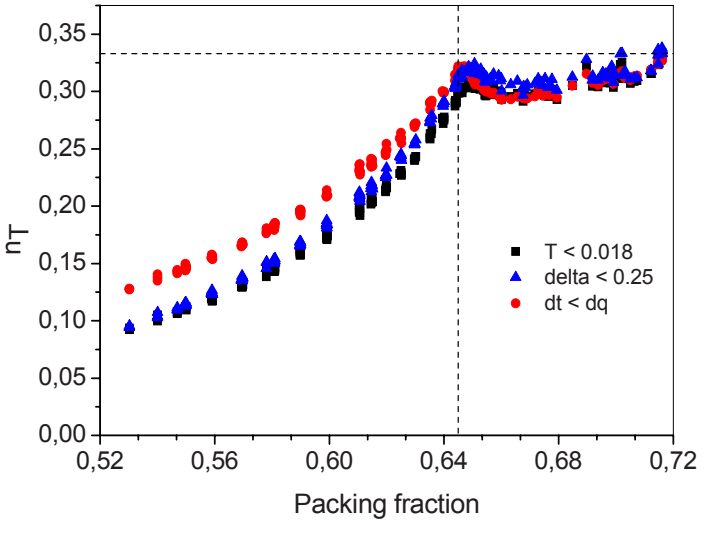


**Fig. 2.12.** Fraction of Delaunay simplexes with tetrahedral shape in packings of hard spheres as a function of packing density. Different curves correspond to different methods for selecting tetrahedra, see Section 2. Vertical dashed line corresponds to the Bernal's limiting density η = 0.645. Horizontal dashed line marks the value of 1/3 that corresponds to the fraction of tetrahedra in the densest fcc and hcp crystals.

tetrahedral configurations [Bernal64, FinneyW]. The further increase in density has little effect on the fraction of tetrahedra. Note that the supremum value is close to 1/3, which corresponds to the fraction of tetrahedra in the densest crystalline structures. The fact that the conditions used for characterizing tetrahedra yield the "crystalline" fraction of tetrahedra at Bernal's limiting density remains unexplained.

Note the Procrustean distances with condition $d_t<d_q$ select a somewhat overestimated fraction of tetrahedra at lower densities. This is because this criterion can pick rather distorted simplexes that are far away from perfect tetrahedron, and are even farther from perfect quartoctahedron.

Fig. 2.13 shows the fraction of Delaunay simplexes selected as quartoctahedra, $n_Q$. The number of these simplexes is greater than of that of tetrahedra at any density. It can seem strange for disordered packings because quartoctahedra are not an "optimal" configuration contrary to the tetrahedron, which is locally a denser and more "stable" configuration. The high population of quartoctahedra can be explained by a statistical reason. Indeed, a simplex with one edge longer than others appears more probable (can be realized by more ways) then a simplex with approximately identical edges. However, the quartoctahedron becomes a preferred configuration at the beginning of crystallization. Indeed, the crystal structure contains tetrahedra adjacent by edges, and just this arrangement of the tetrahedra begets quartoctahedra between them, see Fig. 2.13, right. Thus, the appearance of crystal nuclei in the packings results

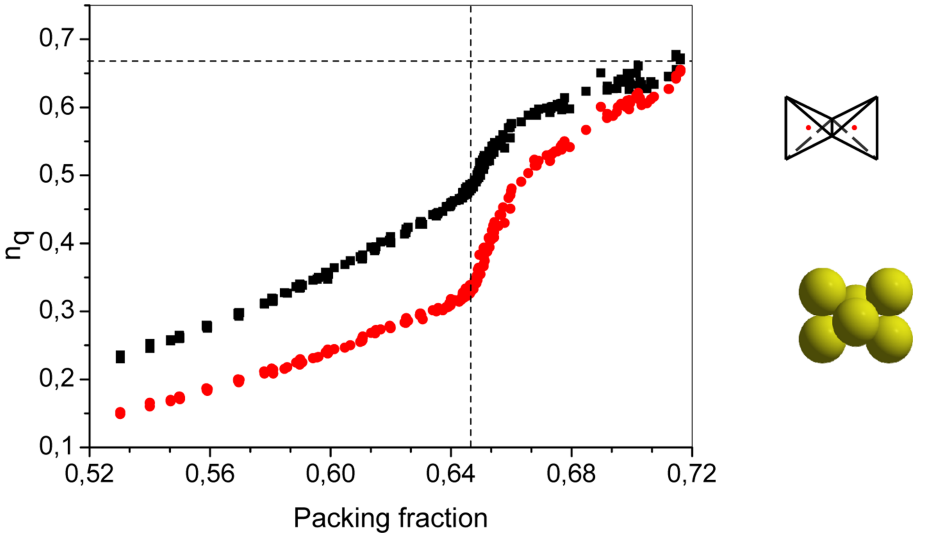


**Fig. 2.13.** Fraction of Delaunay simplexes with quartoctahedral shape in packings of hard spheres as a function of packing density. Different curves correspond to different methods of selecting quartoctahedra: upper curve: $Q < 0.14$, lower curve: $d_Q < 0.897$, see Section 2. Horizontal dashed line marks the value of 2/3 that corresponds to the fraction of quartoctahedra in the densest hcp and fcc crystals. At right: a fragment of fcc structure. It illustrates edge-adjacent tetrahedra and quartoctahedral gaps between them.

inevitably in increase of quartoctahedra ratio. One can see the fastest growth of the curves in Fig.2.13 is observed at the interval 0.645 - 0.66, where intensive appearance of crystalline phase takes place, see below and [AstePRE].

The above-mentioned structural changes become much more expressive if ratio of tetrahedra and quartoctahedra is examined, see Fig. 2.14. In disordered packings, the value of $n_T/n_Q$ grows with density and reaches approximately 2/3 at the limiting density. This ratio is much greater than that in the densest crystal packings, where it is equal to 1/2. Thus the densification of disordered packings is realized predominantly by increasing the ratio of tetrahedral simplexes. Past the limiting density, the ratio drops sharply and reaches the crystalline value somewhere at packing fraction of 0.66-0.67. Past that density, the ratio does not change, which indicates that a "total" crystalline structure has appeared.

In [Med2006] we estimated the maximum of $n_T/n_Q$ at 0.6455 ±0.0015 using measures $T$ and $Q$ for selecting families of Delaunay simplexes. Now we can see that Procrustean distance gives practically the same value of the maximum. It can be clearly seen that limiting density is greater than the widely used value 0.64 and definitely less than 0.65. In [AnikPRL] it was estimated at 0.646.

Every point in Figures 2.12-2.14 represents an individual packing from our set of packings. The fact that one can see more points in Fig.2.14 than in Figs. 2.12 and 2.13 has a trivial explanation that the ratio is more sensitive to fluctuations then the values themselves. Variations of values $n_T$ and $n_Q$ for our packings with the same density are rather small and many points in Figs. 2.12 and 2.13 overlap.

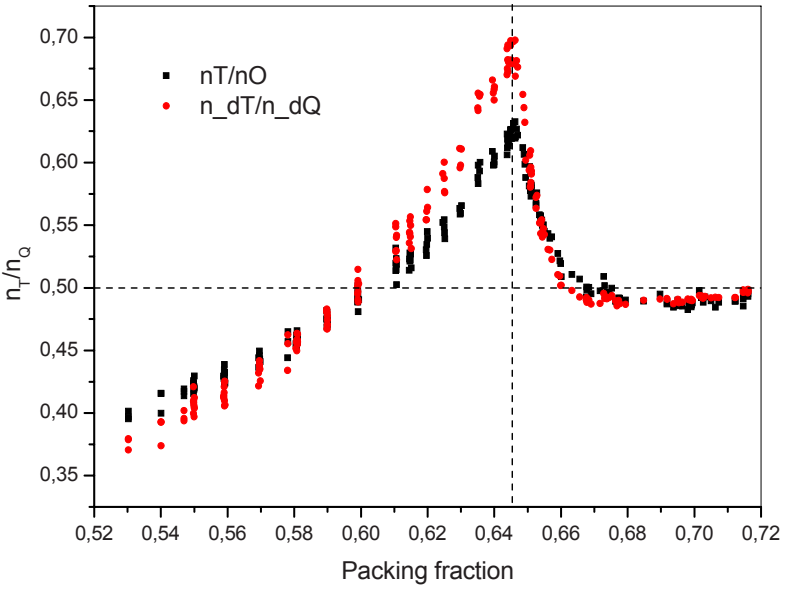


**Fig. 2.14.** Ratio of fraction of tetrahedra $n_T$ to quartoctahedra $n_Q$ in packings of hard spheres as function of packing density. Horizontal line shows 1/2 : a value of this ratio for the densest crystals.

### 2.4.4 Crystallization in Hard Sphere Packings

Here we study crystalline structures in our packings of hard spheres. For this purpose we use structural types of Delaunay simplexes discussed in Section 2.3 (Delaunay simplexes with their surroundings).

Fig.2.15 shows the fraction of volume occupied by the simplexes of crystalline structural types as a function of packing density. Separate curves for FCC and HCP structures, and also the aggregate curve (together with disputed crystalline simplexes, see Section 2.3), are presented. The aggregate curve demonstrates the total volume fraction of "crystalline phase" in packings. Starting from the Bernal's limiting density the fraction of crystal types simplexes increases drastically, which is a direct consequence of crystallization process. In the densest packing (at packing fraction ~0.71) the crystalline phase reaches 95%. The remaining volume belongs to defects in the crystal structure.

One can see a large spread of points on curves for FCC and HCP structures at higher densities. It indicates that these structures may be present in different proportions in packings at the same density. They can exist as separated areas as well as a common crystal with different stacking of layers [AsteW]. In contrary, the aggregation curve is sufficiently smooth at these densities, Fig. 2.15.

Note an inflection of curves at density around 0.66. This peculiarity indicates that the nature of structure transformation is changed. Specifically, at this density the total crystalline order arises replacing independent crystalline nuclei.

At lower densities the fraction of Delaunay simplexes of FCC-type is negligible, up to Bernal's density. At the same time the simplexes of HCP-type are present in

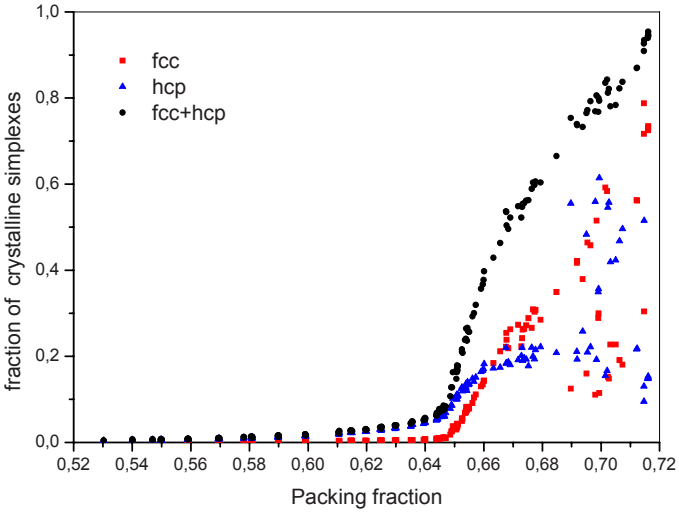


**Fig. 2.15.** Volume fraction occupied by Delaunay simplexes of different structural types as a function of packing density. From bottom to top: fcc-type, hcp-type, accumulative (fcc+hcp+ disputed), see Section 2.3.

small amount (a few percent) in disordered packings. However, this does not indicate the presence of the HCP nuclei. Additional analysis has shown that these simplexes are distributed over the packing without forming compact clusters [Anik_ZSX]. The appearance of HCP-type simplexes in disordered packings can be explained by the existence of face-adjacent tetrahedra which are present in large numbers in these packings (see the next Section).

Fig. 2.16 demonstrates the location of Delaunay simplexes of FCC-type in our models at different densities. As was discussed in Section 2.2.1, the points show the centers of the selected simplex, and the segments connect neighboring centers. Thus, a separated segment represents a pair of adjacent simplexes of FCC-type, and a more complex cluster indicates an aggregate proper to the FCC structure.

The center of a Delaunay simplex is a site of a Voronoi network, and the mentioned segments are edges of this network [Med_book, Naber91, Med88]. Thus, speaking mathematically, we construct an "FCC-coloring" of the Voronoi network. The colored clusters represent patterns of the FCC-structures in the packings.

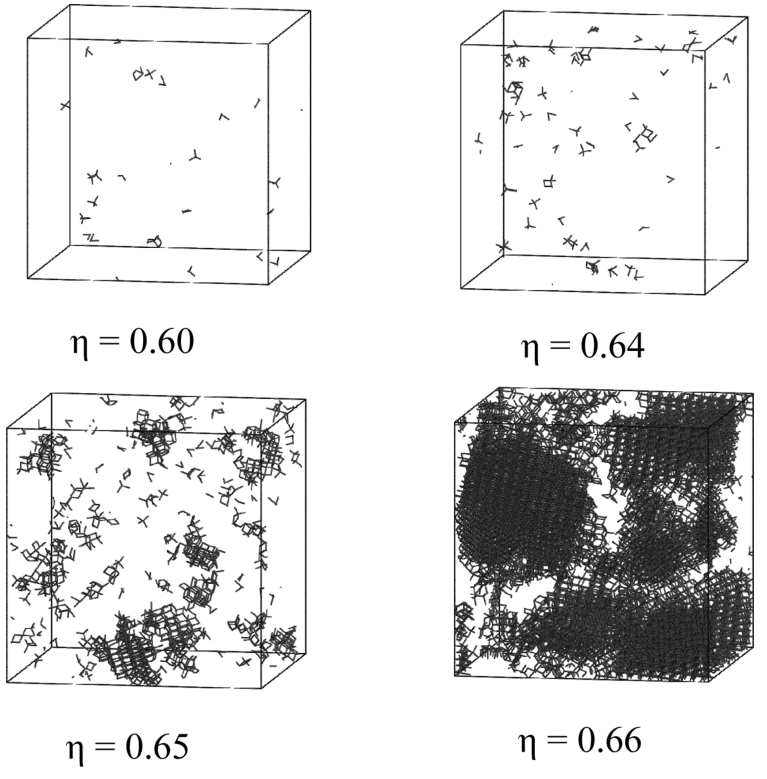


**Fig. 2.16.** Spatial distribution of Delaunay simplexes of fcc-type in packing of hard spheres with different density

One can see that the transformation of the structure takes place at a narrow interval of densities. Indeed, in the interval from 0.60 to 0.64 there are only a few clusters of simplexes of the FCC-type, while at 0.65, the crystal nuclei become clearly visible, and past 0.66, the "crystal phase" dominates.

The analysis of the crystalline structure types of the Delaunay simplexes indicates that our disordered packings do not contain crystalline regions. The small clusters visible at up to Bernal's density are rather random events, and cannot be consider as crystal nuclei.

Per Fig. 2.11, the pair correlation function *g(r)* for packing with 0.65 density had no visible demonstrations of crystallization. Yet Fig. 2.16 clearly shows crystal nuclei at this density.

### 2.4.5 Polytetrahedra

In this Section we consider structure of disordered packings in more detail. A significant feature of such packings is the large fraction of tetrahedral configurations, see Section 2.4.3. They comprise approximately one third of a sample in the densest disordered packings. It is also known that tetrahedral configurations tend to join by faces, forming polytetrahedral aggregates incompatible to lattices [Bernal64, FinneyW, AnikPRL]. We present the analysis of such structures in this Section.

The class of polytetrahedral aggregates (polytetrahedra) includes clusters comprising three or more face-adjacent tetrahedra, see Fig. 2.17. Isolated tetrahedra and pairs of tetrahedra (bipyramids) are omitted as they are found in FCC and HCP crystalline structures. The polytetrahedra can form branching chains, five-member rings, and, in general, a great number of complex aggregates combining such chains and rings.

Fig. 2.18 shows the fraction of tetrahedra involved in the polytetrahedra as a function of packing density. The behavior of these curves is quite different from the

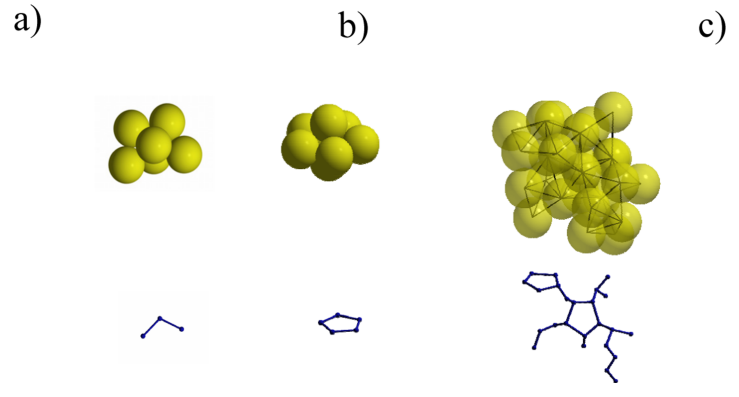


**Fig. 2.17.** Examples of polytetrahedral aggregates (clusters of face-adjacent tetrahedra). (a) – three tetrahedra, b) – a ring of five tetrahedra, c) – a cluster typical for dense disordered packing. The lower row shows the motives of tetrahedra in these aggregates: the points mark the centers of tetrahedra and the lines indicate that they are adjacent through a common face.

curves for total tetrahedra shown in Fig. 2.12. For disordered packings a similarly rapid growth is observed. Upon approaching the limiting Bernal's density they also account for about 30% of the sample volume. Thus, practically all tetrahedra in the packing have coalesced into polytetrahedral aggregates by this density. However, past the limiting density the fraction of polytetrahedra sharply decreases. This is an obvious consequence of forming FCC and HCP nuclei, where tetrahedra tend to have neighbors through their edges or form bipyramids. The Lambda-like behavior of the curves in Fig.2.18 reminds of the ratio of tetrahedra and octahedra (see Fig. 2.14). Both these figures reflect the same fact: the beginning of intensive crystallization just past the limiting density. However, now we can say more about the nature of these structural transformations.

Thus, at limiting density ~0.645 the fraction of tetrahedra reaches its maximum and the polytetrahedral aggregates span their largest extension. A question then arises: why this mechanism stops working at higher densities? Which resource of packing becomes exhausted upon approaching the limiting density? The answer to these questions might be found in Fig. 2.19, which demonstrates that a parameter reaching its limit is the number of spheres involved in tetrahedra [AnikPRL]. For each packing we counted all spheres that are a vertex of at least one tetrahedron. (Recall that each sphere of the packing is a common vertex for several Delaunay simplexes.) As one can see, the fraction of these spheres grows with increasing density and reaches 100% at the limiting density. At this point all spheres in the packing have been involved into the formation of tetrahedra. So the process of densification by means of formation of polytetrahedral nuclei becomes exhausted.

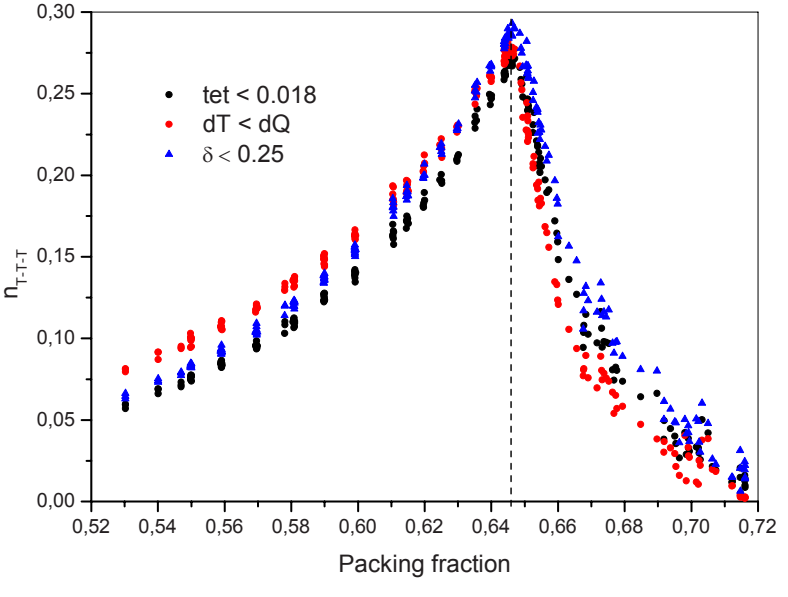


**Fig. 2.18.** Fraction of Delaunay simplexes involved in polytetrahedral aggregates as a function of packing density. Different curves correspond to different methods for selecting tetrahedra.

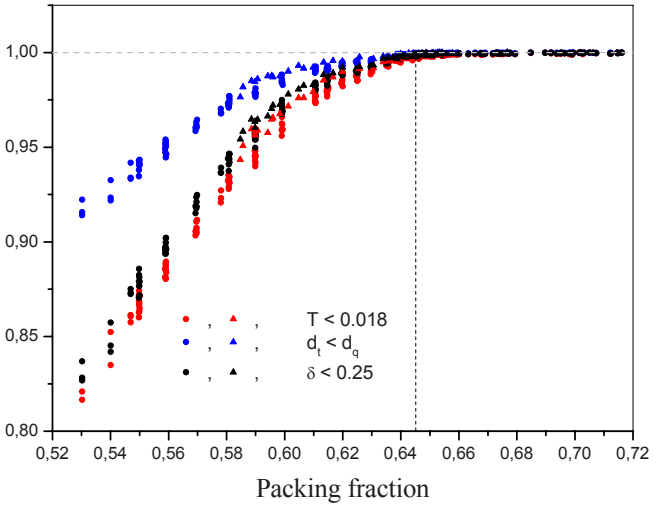


**Fig. 2.19.** Fraction of spheres in the packing involved in quasi-perfect tetrahedra as a function of packing density

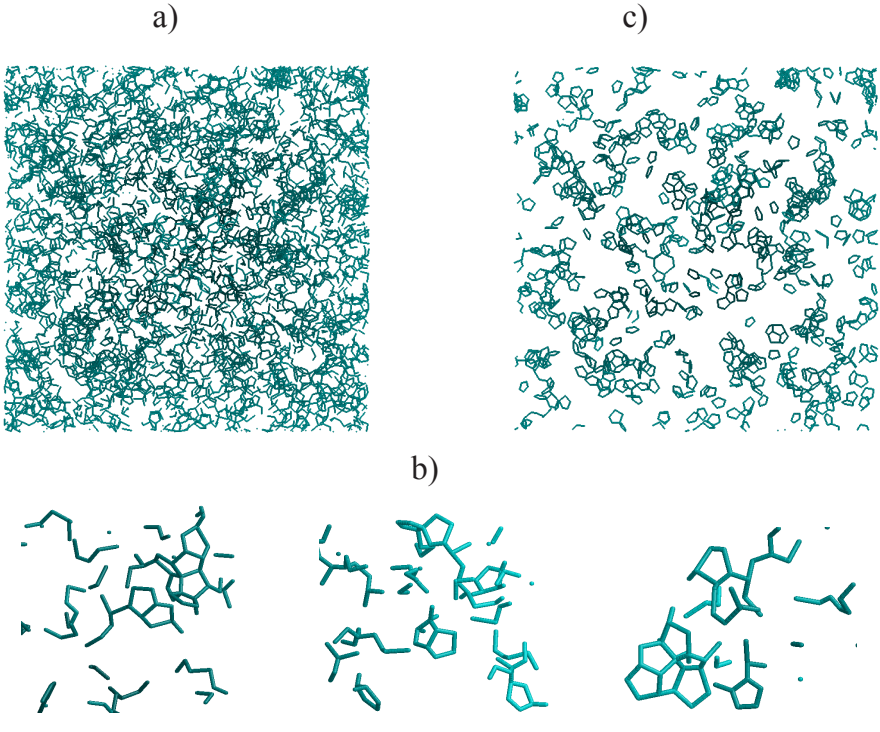


**Fig. 2.20.** Motifs of polytetrahedra on the Voronoi network for a packing of hard spheres with packing fraction ~0.64. (2D projection of the 3D pictures). All clusters selected by the measure T<0.018 (a); small fragments from the picture (b); skeletons of the polytetrahedral clusters (c).

The patterns of spatial distribution of polytetrahedra in the packings can be investigated on the Voronoi network as it was illustrated in Fig. 2.16 where the patterns of crystal clusters were demonstrated (see also Section 2.2.1 and [Med88, Naber91]). However, in this case we select (color) the sites of the Voronoi network, which correspond to Delaunay simplexes belonging to polytetrahedral clusters. Fig. 2.20a presents all polytetrahedra in a packing with density close to the limiting density (~0.640) selected according the measure $T < 0.018$. A detailed examination of the picture reveals that they are comprised of lineal clusters with five-member rings (see Fig. 2.20b where small fragments from different places of Fig. 2.20a are shown at large scale). For lightening the Fig. 2.20a, we have cut off all dead lines of the clusters and also eliminated lineal clusters. The obtained "skeletons" of polytetrahedra are shown in Fig. 2.20c. Here, five-member rings and aggregates of them can be observed. This illustrates an old proposition [Bernal64, Finney70, Med90] that the five-member ring (circle of five tetrahedra, see Fig. 2.17b) is a remarkable feature of dense packings of spheres.

### 2.4.6 Conclusions about Structure of Hard Sphere Packings

We reported results of our analysis of a set of identical hard sphere packings in a broad interval of densities. Our packings are not abstract constructions realizing a given density. They are "statistically preferable" configurations obtained by densification from randomly distributed spheres. They can represent a pouring of spherical beads, atomic systems like liquids and glasses, intervening medium between glasses and crystals, and defective crystals. Our task is to understand which kind of the structure is more preferable to realize a given density. The performed analysis reveals properties of packings, and gives helpful information for understanding the structure of atomic systems. Our packings are quite representative, i.e. the packings having the same density possess statistically equivalent structure.

We confirm that the non-crystalline packings can exist at up to Bernal's limiting packing density of ~0.64 (we propose a more precise estimation 0.645-0.646). It is justified by the detailed analysis of the Delaunay simplexes, which show the lack of crystal nuclei in packings up to this density. However, the disordered packings are in no way random. They contain some specific local configurations. One can select a class of Delaunay simplexes with the shape close to a regular tetrahedron, and another class of the simplexes with the shape close to a regular quartoctahedron. The total fraction of these simplexes increases with density and, at the Bernal's limit, becomes more than 70%. At that density, the ratio between tetrahedra and quartoctahedra reaches 2/3, which is substantially larger than the ratio for the densest crystalline packings, where its value is 1/2.

The analysis of mutual arrangements of Delaunay simplexes has shown that the tetrahedra tend to cluster by their faces forming a variety of aggregates (polytetrahedra), which have a rather high local density, and are incompatible with lattices. One can say that polytetrahedral principle of the structure is realized in dense disordered packings. Such structure seems very natural. Indeed, a tetrahedron is the densest local configuration, which should be present in any dense packing of spheres. An additional sphere can be placed at a face of the tetrahedron forming an adjacent tetrahedral configuration. Further, a new sphere can be positioned at any face of either the new or the

original tetrahedron, with the derived aggregate forming the next adjacent tetrahedron. Thus, the formation of polytetrahedra is a spontaneous process, which can explain why this structural principle is always realized at pouring of spheres. The formation of such configurations seems geometrically more probable than crystalline ones. Polytetrahedra can explain a phenomenon of supercooling of one-atomic liquids [Frank]. As mentioned, they have a relatively high local density (it means they can be rather stable), and extrinsic for crystals (which means they have a barrier to turn into crystal). All of these can prevent homogeneous crystallization of liquids.

The following questions deserve special attention. Why the polytetrahedral principle cannot generate density higher then ~0.645? What is the resource of the packing that becomes exhausted upon approaching the limiting density? This problem still remains a challenge for both physicists and mathematicians. It represents "the disordered analogue" of the Kepler conjecture for the densest crystalline packing of spheres. We demonstrated that one of the parameters reaching its limit is the number of spheres involved in formation of the tetrahedra. Thus, the increase in the density of a disordered packing occurs through an increase in the number of tetrahedral configurations that coalesce into polytetrahedra. This process is sustained by involving more and more spheres into tetrahedra. However, after all spheres of the system have been exhausted, a further densification would require another mechanism to increase the density of the packing.

Packings with density higher then Bernal' limiting density necessarily contain crystal structures. We have observed nuclei comprising hundreds of spheres in packings with density 0.65. The number of nuclei and their size increase drastically with the growth of packing density. Thus, in packings with 0.66, the main part of the sample has a crystalline structure. Further densification is realized by the forming of a "total" crystal and by improving the quality of the crystalline phase (decrease of defects and perfecting of local structure).

## 2.5 Conclusion

We apply Delaunay simplexes to investigation of the structure of dense packings of hard spheres. Delaunay simplexes are a powerful tool of the computer geometry, which allows to tackle structure problems that are difficult for other methods of analysis, such as the method of correlation functions. Delaunay simplexes can be characterized by different structure parameters, including simplex shape and the structural type. Clusters of such simplexes reveal structural patterns in packings. They help to clarify the structure of homogeneous disordered (non-crystalline) systems as well as to study the appearance of crystalline nuclei.

Different methods for characterization of simplex shapes were discussed. A measure of shape is the proximity of a simplex shape to a reference shape. The mathematical theory of shape proposes to use the Procrustean distance for this purpose. It is defined as a mean square deviation between vertices of the simplexes at the optimal superposition of a given simplex on a reference one. Simpler methods use lengths of simplex edges. We discussed the measures of "tetrahedrisity" and "quartoctahedrisity" proposed in physics to select families of simplexes close to regular tetrahedra and to a fourth of octahedron. Here, an invariant of the lengths is constructed, which

has a zero value for an etalon simplex shape. In the simplest case the length of the maximal edge can be used to estimate proximity to regular tetrahedron. This characteristic was proposed by Hales in his proof of the Kepler conjecture. However, it was shown that the different measures are not critical for structural analysis of packings of spheres.

Besides the Delaunay simplex shape, a new characterization – the structural type – was also considered. It had to be introduced because a single simplex (four atoms) does not define the structure unambiguously, e.g. a simplex of tetrahedral shape is present in both FCC and HCP structures, and also in dense disordered packings. Thus it was proposed to take neighbor simplexes into account. Then it becomes easy to reveal crystal nuclei and to calculate the fraction of crystal phase in a packing.

The application of this geometric approach to study structure of hard sphere packings was presented. Computer models of dense packings of identical hard spheres in a wide range of densities were generated. It was shown that a characteristic feature of a disordered packing is its polytetrahedral structure, i.e. the packing contains an appreciable fraction of tetrahedral configurations that tend to coalesce through their faces to form locally dense aggregates of various morphology, incompatible with translational symmetry. The obtained results can help to understand the structure of liquids, solid amorphous phase, colloidal systems and granular matter.

## Acknowledgements

This work was supported by grants from Russian Foundation for Basic Research No. 05-03-032647, no. 08-03-00140, and partly from YS INTAS no. 04-83-3865 (to A.A.), Alexander von Humbold Foundation (N.M.): and NSERC Granting Agency, Canada.

## References

[AsteW] Aste, T., Weaire, D.: The Pursuit of Perfect Packing (Institute of Physics, Bristol 2000)

[Hales5] Hales, T.C.: A proof of the Kepler conjecture. Annals of Mathematics 162, 1065–1185 (2005)

[Conway] Conway, J.H., Sloane, N.J.A.: Sphere Packings, Lattices and Groups. Springer, New York (1988)

[phys_liq] Temperley, H.N.V., Rowlison, J.S., Rushbrooke, G.S.: Physics of simple liquids. Noth-Holland Pub.Company, Amsterdam (1968)

[Croxton] Croxton, C.A.: Liquid state physics – a statistical mechanical introduction. Cambridge Univ. Press, Cambridge (1974)

[Hansen] Hansen, J.P., McDonald, I.R.: Theory of Simple Liquids, 3rd edn. Academic press, Amsterdam (2006)

[colloid_exp]van Blaaderen, A., Wiltzius, P.: Real-Space structure of colloidal hard-sphere glasses. Science 270, 1177–1179 (1995)

[Gasser] Gasser, U., Schofield, A., Weitz, D.A.: Local order in a supercooled colloidal fluid observed by confocal microscopy. J. Phys. Condence. Matter 15, S375–S380 (2003)

[Aste_exp] Aste, T., Saadatfar, M., Senden, T.J.: Geometrical structure of disordered sphere packings. Phy. Rev. E 71, 61302 (2005)

[Voronoi] Voronoi, G.F.: Nouvelles applications des parametres continus a la theorie des formes quadratiques. Deuxieme Memorie: Recherches sur les paralleloedres primitifs. J. Reine Angew Math. 136, 67 (1909)

[Delaunay] Delaunay, B.N.: Sur la sph‘ere vide. A la memoire de Georges Voronoi. Izv Akad Nauk SSSR Otd Mat i Estestv nauk 7, 793 (1934)

[Okabe] Okabe, A., Boots, B., Sugihara, K., Chiu, S.: Spatial tessellations - concepts and applications of Voronoi diagrams. Wiley, New-York (2000)

[Med_book] Medvedev, N.N.: Voronoi-Delaunay method for non-crystalline structures. SB Russian Academy of Science, Novosibirsk (2000) (in Russian)

[Finney70] Finney, J.L.: Random packings and the structure of simple liquids. I. The geometry of random close packing. Roy. Soc. London 319, 479–494 (1970)

[Malley] O'Malley, B., Snook, I.: Crystal nucleation in the hard sphere system. Phys. rev. Lett. 90, 85702 (2003)

[Bosticka] Bosticka, D., Vaisman, I.I.: A new topological method to measure protein structure similarity. Biochem. and Biophys. Res. Comm. 304, 320–325 (2003)

[Alinchenko] Alinchenko, M.G., Anikeenko, A.V., Medvedev, N.N., Voloshin, V.P., Mezei, M., Jedlovszky, P.: Morphology of voids in Molecular Systems. A Voronoi-Delaunay analysis of a simulated DMPC membrane. J. Phys. Chem. B 108, 19056 (2004)

[Bryant] Bryant, S., Blunt, M.: Prediction of relative permeability in simple pore media. Phys. Rev. 46(4), 2004–2011 (1992)

[Naber91] Naberukhin, Y.I., Voloshin, V.P., Medvedev, N.N.: Geometrical analysis of the structure of simple liqids: percolation approach. Mol. Phys. 73(4), 917–936 (1991)

[Med88] Medvedev, N.N., Naberukhin Yu., I.: Structure of simple liquids as a percolation problem on the Voronoi network. J. Phys. A: Math. Gen. 21, L247–L252 (1988)

[Vol95] Voloshin, V.P., Naberukhin, Y.I., Medvedev, N.N., Jone, M.S.: Investigation of free volume percolation under the liquid-glass phase transition. J. Chem. Phys. 102, 4981–4986 (1995)

[Naber91] Naberukhin, Y.I., Voloshin, V.P., Medvedev, N.N.: Geometrical analysis of the structure of simple liqids: percolation approach. Mol. Phys. 73(4), 917–936 (1991)

[Gellatly] Gellatly, B.J., Finney, J.L.: Characterisation of models of multicomponent amorphous metals: the radical alternative to the Voronoi polyhedron. J. Non-Cryst. Solids 50, 313–329 (1982)

[Aurenhammer87] Aurenhammer, F.: Power diagrams: properties, algorithms and applications. SIAM Journal on Computing 16(1), 78–96 (1987)

[Gavrilova97] Gavrilova, M., Rokne, J.: An efficient algorithm for construction of the power diagram for the Voronoi diagram in plane. Int. J. Comput. Math. 61, 49–61 (1997)

[Telley] Telley, H., Liebling, T.M., Mocellin, A.: The Laguerre model of grain growth in two dimensions I. Cellular structures viewed as dynamical Laguerre tessellations. Philosophical Magazine B 73(3), 395–408 (1996)

[Edelsbruner84] Aurenhammer, F., Edelsbruner, H.: An optimal algorithm for construction the weighted Voronoi diagram in the plane. Pattern Recognition 17(2), 251–257 (1984)

[Gavrilova] Gavrilova, M.: A Reliable Algorithm for Computing the Generalized Voronoi Diagram for a Set of Spheres in the Euclidean d-dimensional Space. In: Proceedings of the 14th Canadian Conference on Computational Geometry, August, Lethbridge, Canada, pp. 82–87 (2002)

[Kim] Kim, D.-S., Cho, Y., Kim, D.: Euclidean Voronoi diagram of 3D balls and its computation via tracing edges. Computer-Aided Design 37(13), 1412–1424 (2005)

[Med95] Anishchik, S.V., Medvedev, N.N.: Three-dimensional Apollonian packing as a model for dense granular systems. Phys. Rev. Lett. 75(23), 4314–4317 (1995)

[Med06] Medvedev, N.N., Voloshin, V.P., Luchnikov, V.A., Gavrilova, M.L.: An algorithm for three-dimensional Voronoi S-network. J. of Comput. Chem. 27(14), 1676–1692 (2006)

[Kendall] Kendall, D.G., Barden, D., Carne, T.K., Le, H.: Shape and shape theory. Wiley, Chichester (1999)

[Small] Small, C.: The statistical theory of shape. Springer, New York (1996)

[Anik2006] Anikeenko, A.V., Medvedev, N.N., Gavrilova, M.L.: Application of Procrustes Distance to Shape Analysis of Delaunay Simplexes. In: Werner, B. (ed.) Proceedings of the 3rd International Symposium on Voronoi Diagrams in Science and Engineering 2006, pp. 148–152. IEEE Computer Society, Los Alamitos (2006)

[Kimura] Kimura, M., Yonezawa, F.: Nature of amorphous and liquid structures—computer simulations and statistical geometry. J. Non-Cryst. Solids 535, 61–62 (1984)

[Med87] Medvedev, N.N., Naberukhin, Y.I.: Shape of the Delaunay simplices in dense random packings of hard and soft spheres. J. Non-Cryst. Solids 94, 402–406 (1987)

[Debene] Lynden-Bell, R.M., Debenedetti, P.: Computational Investigation of Order, Structure, and Dynamics in Modified Water Models. J. Phys. Chem. B 109(14), 6527–6534 (1987)

[Med86] Medvedev, N.N., Naberukhin, Y.I.: Delaunay simplices of simple liquid and amorphous materials. Dolkady Akad.Nauk USSR 288(5), 1104–1107 (1986) (in Russian)

[Dompierre] Dompierre, J., Vallet, M.-G., Labbé, P., Guibault, F.: An analysis of simplex shape measures for anisotropic meshes. Computer Methods in Applied Mechanics and Engineering 194(48-49), 4895–4914 (2005)

[Hales97] Hales, T.C.: Sphere packings, I. Discrete Comput. Geom. 17, 1–51 (1997)

[Anik_Jap] Anikeenko, A.V., Gavrilova, M.L., Medvedev, N.N.: The coloring of the Voronoi network: investigation of structural heterogeneity in the packings of spheres. Japan J. Indust. Appl. Math. 22, 151–165 (2005)

[Brov] Oleinikova, A., Brovchenko, I.: Percolating networks and liquid–liquid transitions in supercooled water. J. Phys. Condens. Matter 18, S2247–S2259 (2006)

[Vol89] Voloshon, V.P., Naberukhin, Y.I., Medvedev, N.N.: Can various classes of atomic configurations (Delaunay simplices) be distinguished in random dense packing of spherical particles? Mol. Simulation 4, 209–227 (1989)

[Dryden] Dryden, I.L., Mardia, K.: Statistical Shape Analysis. John Wiley & Sons, New York (1998)

[Eggert] Eggert, D., Lorusso, A., Fisher, R.B.: Estimating 3-D Rigid Body Transformations: A Comparison of Four Major Algorithms. Machine Vision and Applications 9, 272–290 (1997)

[Umeyama] Umeyama, S.: Least-squares estimation of transformation parameters between two point patterns. IEEE Transactions on Pattern Analysis and Machine Intelligence 13(4), 378–380 (1991)

[AnikPRL] Anikeenko, A.V., Medvedev, N.N.: Polytetrahedral Nature of the Dense Disordered Packings of Hard Spheres. PRL 98, 235504 (2007)

[Anik_LNCS] Anikeenko, A.V., Gavrilova, M.L., Medvedev, N.N.: A novel Delaunay simplex technique for detection of crystalline nuclei in dense packings of spheres. In: Gervasi, O., Gavrilova, M.L., Kumar, V., Laganá, A., Lee, H.P., Mun, Y., Taniar, D., Tan, C.J.K. (eds.) ICCSA 2005. LNCS, vol. 3480, pp. 816–826. Springer, Heidelberg (2005)

[Anik_ZSX] Anikeenko, A.V., Medvedev, N.N.: Homogeneous crystallization of the Lennard-Jones liquid. Structural analysis based on Delaunay simplices method. Journal of Structural Chemistry 47(2), 267–276 (2006)

[Bernal59] Bernal, J.D.: A geometrical approach to the structure of liquids. Nature 183, 141–147 (1959)

[Bernal60] Bernal, J.D.: Geometry of the structure of monatomic liquids. Nature 185, 68–70 (1960)

[Bernal64] Bernal, J.D.: The Bakerian lecture, 1962. The structure of liquids. Proc. R. Soc. Lond. A 280, 299–322 (1964)

[Onoda] Onoda, G.Y., Liniger, E.G.: Random loose packings of uniform spheres and the dilatancy onset. Phys. Rev. Lett. 64, 2727–2730 (1990)

[Aste05] Aste, T.: Variations around disordered close packing. J. Phys. Condens. Matter 17, S2361–S2390 (2005)
[FinneyW] Finney, J.L., Wallace, J.: Interstice correlation functions: a new, sensitive characterization of non-crystalline packed structures. J. Non-Cryst. Solids 43, 165–187 (1981)
[Med90] Medvedev, N.N.: Aggregation of tetrahedral and quartoctahedral Delaunay simplices in liquid and amorphous rubidium. J. Phys. Condens. Matter 2, 9145–9154 (1990)
[AstePRE] Anikeenko, A.V., Medvedev, N.N., Aste, T.: Structural and entropic insights into the nature of random close packing limit. Phys. Rev. E 77, 31101 (2008)
[Frank] Frank, F.C.: Supercooling of liquids. Proc. R. Soc. London. A 215, 43–46 (1952)
[Reichert] Reichert, H., et al.: Observation of five –fold local symmetry in liquid lead. Nature 408, 839–841 (2000)
[Schenk] Schenk, T., Holland-Moritz, D., Simonet, V., Bellissent, R., Herlach, D.M.: Icosahedral short -range order in deeply undercooled metallic melts. Phys. Rev. Lett. 89(7), 75507 (2002)
[Scott69] Scott, G.D., Kilgour, D.M.: The Density of Random Close Packing of Spheres. Brit. J. Appl. Phys (J. Phys. D) 2, 863–869 (1969)
[Jodrey] Jodrey, W.S., Tory, E.M.: Computer simulation of close random packing of equal spheres. Phys. Rev. A 32, 2347–2351 (1985)
[Clarke] Clarke, A., Jonsson, H.: Structural changes accompanying densification of random hard-sphere packings. Phys Rev. E 47(6), 3975–3984 (1993)
[Rintoul] Rintoul, M.D., Torquato, S.: Hard-sphere statistics along the metastable amorphous branch. Phys. Rev. E 58(1), 532–537 (1998)
[Med2006] Anikeenko, A.V., Medvedev, N.N., Elsner, A., Lochmann, K., Stoyan, D.: Critical densities in hard sphere packings. Delaunay simplex analysis. In: Proc.of the 3rd Inter. Symp. Voronoi Diagrams in Science and Engin. 2006, pp. 153–158. IEEE Computer Society, Los Alamitos (2006)
[Torquato2000] Torquato, S., Truskett, T.M., Debenedetti, P.G.: Is random close packing of spheres well defined? Phys. Rev. Lett. 84(10), 2064–2067 (2000)
[Richard99] Richard, P., Oger, L., Troadec, J.-P., Gervois, A.: Geometrical characterization of hard-sphere systems. Phys. Rev. E 60(4), 4551–4558 (1999)
[ZSX07] Anikeenko, A.V., Medvedev, N.N.: Structural features of dense hard-sphere packings. Critical densities. Zhurnal Strukturnoi Khimii 48(4), 823–830 (2007) (in russian)
[Kristin] Lochmann, K., Anikeenko, A.V., Elsner, A., Medvedev, N.N., Stoyan, D.: Statistical verification of crystallization in hard sphere packings under densification. Eur. Phys. J. B 53, 67–76 (2006)
[Hoover] Hoover, W.G., Ree, F.H.: Melting transition and communal entropy for hard spheres. J. Chem. Phys. 49, 3609–3617 (1968)
[Auer] Auer, S., Frenkel, D.: Numerical prediction of absolute crystallization rates in hard-sphere colloids. J. Chem. Phys. 120, 3015–3029 (2004)
[Skoge] Skoge, M., Donev, A., Stillinger, F.H., Torquato, S.: Physical Review E. 74, 41127 (2006)